Uluslararası Sürdürülebilir Mühendislik ve Teknoloji Dergisi
International Journal of Sustainable Engineering and Technology
ISSN: 2618-6055 / Cilt: 9, Sayı: 1, (2025), 94 – 106
Araştırma Makalesi – Research Article

INTERACTIVE X-RAY TUBE SIMULATION: A TOOL FOR BIOMEDICAL EDUCATION

Ali AKYÜZ[1,2*], Durmuş TEMİZ[1]

[1]Burdur Mehmet Akif Ersoy Üniversitesi, Bucak Emin Gülmez Teknik Bilimler Meslek Yüksekokulu, Burdur
[2]Burdur Mehmet Akif Ersoy Üniversitesi, Bucak Bilgisayar ve Bilişim Fakültesi, Burdur

(Geliş/Received: 27.05.2025, Kabul/Accepted: 20.06.2025, Yayınlanma/Published: 30.06.2025)

ABSTRACT

This paper presents an interactive X-ray Tube Simulator designed for students in biomedical engineering and biomedical device technology. Developed using HTML, CSS, and JavaScript and integrating the Chart.js library for dynamic graphical representations, this simulator offers dynamic visualizations and real-time graphical analysis to understand X-ray tube operation comprehensively. The simulator allows users to select tube voltage (kV), filament current (mA), exposure time (ms), anode angle (°), anode rotation speed (RPM), anode material (Tungsten, Molybdenum, Rhodium), cathode thickness (mm), filter thickness (mm), filter material (Aluminum, Copper, Molybdenum), collimator aperture (mm), chamber distance (cm), glass type (Lead, Borosilicate) and cooling type (Oil, Water), Air) and instantly observe their effects on X-ray spectra, radiation dose, heat accumulation and energy efficiency. This tool aims to bridge the gap between theoretical knowledge and practical application, promoting a deeper understanding of X-ray physics and safety considerations in a safe and cost-effective environment.

Keywords: Simulation, X-ray, Education, Biomedical

ETKİLEŞİMLİ X-IŞINI TÜPÜ SİMÜLASYONU: BİYOMEDİKAL EĞİTİM İÇİN BİR ARAÇ

ÖZ

Bu çalışma, biyomedikal mühendisliği ve biyomedikal cihaz teknolojisi öğrencileri için tasarlanmış etkileşimli bir X-Işını Tüpü Simülatörü sunmaktadır. HTML, CSS ve JavaScript kullanılarak geliştirilen ve dinamik grafiksel gösterimler için Chart.js kütüphanesini entegre eden bu simülatör, X-ışını tüpü operasyonunun kapsamlı bir şekilde anlaşılmasını sağlamak amacıyla dinamik görselleştirmeler ve gerçek zamanlı grafik analizleri sunar. Simülatör, kullanıcıların tüp voltajı (kV), flaman akımı (mA), maruz kalma süresi (ms), anot açısı (°), anot dönüş hızı (RPM), anot materyali (Tungsten, Molibden, Rodyum), katot kalınlığı (mm), filtre kalınlığı (mm), filtre materyali (Alüminyum, Bakır, Molibden), kolimatör açıklığı (mm), oda mesafesi (cm), cam türü (Kurşun, Borosilikat) ve soğutma türü (Yağ, Su, Hava) gibi tüm temel parametreleri manipüle etmelerine ve bunların X-ışını spektrumları, radyasyon dozu, ısı birikimi ve enerji verimliliği üzerindeki etkilerini anında gözlemlemelerine olanak tanır. Bu araç teorik bilgi ile pratik uygulama arasındaki boşluğu doldurmayı, güvenli ve uygun maliyetli bir ortamda X-ışını fiziği ve güvenlik hususlarının daha derinlemesine anlaşılmasını teşvik etmeyi amaçlamaktadır.

Anahtar kelimeler: Simülasyon, X-ışını, Eğitim, Biyomedikal

***Sorumlu Yazar/Corresponding Author:** aakyuz@mehmetakif.edu.tr

ISSN: 2618-6055 / 9, (1), 94 – 106, 2025
DOI: 10.62301/usmtd.1707321

1. Introduction

X-ray technology revolutionized the world of medicine with a chance discovery by Wilhelm Conrad Röntgen in the late 19th century. These high-energy rays of the electromagnetic spectrum serve as a critical tool for non-invasive imaging of the human body. After Röntgen's wife took the first X-ray image, this technology became a unique tool for visualizing the internal structure of organs and tissues. Thanks to X-ray equipment that emits invisible rays, it has become possible to examine our bones and the anomalies in the internal organs in detail. X-rays are one of the most widely used tools for diagnosing diseases, from oncology to occupational health. However, it is important to remember both the potential dangers and the power of X-rays [1-4]. Long-term cell damage and increased risk of cancer can result from high doses of X-ray exposure. X-ray applications should always be carried out cautiously, and unnecessary exposure should be avoided [5]. The amazing discovery of X-rays has saved millions of lives and enabled new ways to diagnose and treat diseases. X-rays are absorbed at certain rates as they pass through solids. The density and atomic structure of the material affect this absorption rate. For example, elements with high atomic numbers absorb more X-rays than soft tissues. These differences create different gradations in X-ray images and give important details about, for example, a patient's internal anatomy. Each tissue appears in a different color, as if touched with a paintbrush; details cannot be missed [6]. X-rays are generated when high-energy electrons collide with a target material, typically tungsten. The electrons lose energy during this collision, and X-rays are generated. These rays are collected on a detector or film to form an image, much like the lens of a camera [7]. To optimize the imaging process, the detector system and X-ray instrument design significantly impact image quality. The X-rays ' wavelength can vary depending on the materials and the targeted area's nature [8]. X-ray technology is becoming increasingly more reliable and efficient thanks to advances in digital systems and image processing methods. With digital X-ray systems providing faster and clearer images at lower doses, patients are exposed to less radiation. Furthermore, by facilitating remote access and storage, image digitization is raising the standard of medical services [9].

In modern healthcare, trained personnel in the biomedical field are very important for device installation, use, repair, and technical service. This field requires careful transfer of scientific knowledge and technical skills in the healthcare sector. It is of great importance in patient safety, treatment effectiveness, and the training of future specialists. Innovations in technology, especially in medical devices, require training that will adapt over time. An important part of this learning process includes simulations [10]. The disadvantages of traditional educational techniques are overcome by simulations that reduce the uncertainty of the real clinical environment, reduce the possibility of error, and provide students with a safe learning environment [11]. In particular, X-ray machine simulations help students understand imaging methods, develop decision-making skills, and understand how medical devices work. Moreover, giving them the chance to practice possible challenges they may encounter during the learning process is a wise investment that will raise the standard of healthcare services in the future. Computer-based simulations are usually conducted through relevant software, allowing users to improve their ability to use X-ray equipment in a virtual environment. The major advantage of such simulations is the huge savings for users in terms of time and cost. Students who learn about the complex settings of X-ray equipment must learn without experiencing errors in the real environment.

In this study, we developed an interactive X-Ray Tube Simulator designed as an educational tool for biomedical engineering and biomedical device technology students. Built using HTML, CSS, and JavaScript, with the Chart.js library for dynamic graphical representations, the simulator integrates dynamic visualizations and real-time graphical analyses to understand X-ray tube operation comprehensively. By allowing users to manipulate key parameters and observe their effects on X-ray spectra, radiation dose, heat accumulation, and energy efficiency, this tool aims to bridge the gap between theoretical knowledge and practical application, fostering a deeper understanding of X-ray physics and safety considerations in a safe and cost-effective environment.

2. Materials and Methods

The simulator was designed with comprehensive and interactive features to provide biomedical device technology engineering and electronics technician students with information about the operating principles of the X-ray tube.

*Sorumlu Yazar/Corresponding Author: aakyuz@mehmetakif.edu.tr

ISSN: 2618-6055 / 9, (1), 94 – 106, 2025
DOI: 10.62301/usmtd.1707321

The user interface was created using HTML5 and CSS3 technologies in a contemporary and interactive manner. While CSS3 controls the interface's visual design and layout, HTML5 ensures that the page structure is arranged meaningfully and systematically. Within the HTML structure, basic elements like canvas elements for graphics, parameter controls (sliders and selection elements), and information boxes for summarizing information are arranged logically in groups.

A responsive and flexible design that adjusts to the simulator's various screen sizes uses contemporary layout techniques like CSS, flexbox, and grid. The color scheme, typefaces, and animation effects have been carefully chosen to improve the user experience and present information more clearly. This makes it simple for users to monitor results and change parameters visually.

JavaScript's ability to dynamically control parameter elements is one of the main features that allows user interaction in the simulator. Sliders representing various settings such as tube voltage (kV), filament current (mA), and exposure time (ms) are retrieved from the HTML structure using the document.getElementById() method and grouped into a JavaScript object (e.g., sliders).

The tab system in the user interface is designed to provide easy access to different analysis and visualization sections - for example, X-ray spectrum, dose analysis, heat analysis, energy analysis, and statistics. In this system, created with JavaScript, when the user clicks on a tab, the content of that tab appears on the screen. To achieve this, the querySelectorAll() method is used to select and loop over all tabs and content sections. While the “active” class is added to the clicked tab, other tabs and content are stripped of this class. Thus, users can easily navigate complex data and quickly access the necessary information.

The HTML5 Canvas API is used to visually represent the physical processes and parts of the X-ray tube. The 2D drawing context (getContext(“2d”)), obtained with JavaScript, enables the animation of dynamic processes such as the movement of electrons from cathode to anode, X-ray generation, anode rotation, and heating. Each physical component (cathode, anode, glass tube, collimator, filtration, etc.) is drawn in specific coordinates and with appropriate colors; visual effects such as color change according to the temperature of the anode are applied.

A realistic animation is achieved by moving electrons and X-rays according to speed and direction parameters. Parameters such as the rotation speed of the anode and temperature are also integrated into the animation. This approach allows students to directly observe the physical phenomena inside the X-ray tube and the effects of parameter changes, and makes abstract concepts concrete.

For the simulator to produce accurate and realistic results, it is critical to accurately describe the physical and electrical properties of the materials used (anode, cathode, glass, filtration, cooling). For this purpose, each material's atomic number (Z), K_α and K_β characteristic energy values, density, heat capacity, melting point, work function, emission efficiency, etc., are stored in JavaScript objects. For example, different properties such as emission efficiency are defined for anode materials (Tungsten, Molybdenum, Rhodium) and similarly for cathode materials (Tungsten, Tungsten with Thorium). This data is used in various calculations such as X-ray spectrum calculations, dose analysis, heat accumulation simulations, and energy efficiency evaluations, ensuring that the simulation produces results close to physical reality.

The simulator applies physical models to analyze the X-ray spectrum. The relative intensity of the beam, electron energy, and filtration effects primarily modulate the Bremsstrahlung spectrum, which is calculated over the energy range by considering the tube voltage (kV) and other factors. The X-ray intensity I is proportional to the electron energy E and the maximum energy Emax and is expressed by $I(E) \propto E(_{Emax}\text{-}E)$. This formula implies that part of the kinetic energy of the electrons is converted into X-rays, and the spectrum is shaped depending on the energy [12]. As the X-ray beam passes through the filtration material, low-energy photons are absorbed. This effect is modeled by the Lambert-Beer law (Equation 1). $I_{filter}(E)$ is the intensity after filtration, $\mu(E)$ is the energy-dependent absorption coefficient that varies with the material, and x is the filtration thickness. In the simulator, the filtration coefficient is approximated by a constant coefficient concerning the material and thickness. The X-ray beam also passes through obstacles such as the glass tube and the cathode thickness. The absorption coefficients similarly model these effects in Equations (2) and (3), where T_{glass} is the transmission coefficient of the

*Sorumlu Yazar/Corresponding Author: aakyuz@mehmetakif.edu.tr

ISSN: 2618-6055 / 9, (1), 94 – 106, 2025
DOI: 10.62301/usmtd.1707321

glass, the absorption coefficient depends on the cathode thickness, d_{cat} is the cathode thickness. E is the energy [13, 14].

$$I_{filter}(E) = I(E)e^{-\mu(E)x} \quad (1)$$

$$I_{glass}(E) = I_{filter}(E)T_{glass} \quad (2)$$

$$I_{cat}(E) = I_{glassr}(E)e^{-\alpha dcat\ E} \quad (3)$$

Focusing cup voltage and tube current fluctuation affect the amplitude of the spectrum. The simulator expresses these effects by coefficients (V_{focus}: Focusing cup voltage, ripple: Percentage of current ripple, k_{focus}: Focusing effect coefficient). It is modeled by Equation (4). Depending on the atomic number of the anode material, characteristic K_α and K_β lines appear at certain energy levels. These lines are added to the spectrum when the tube voltage exceeds these energy levels [15].

$$I_{final}(E) = I_{cat}(E)\ (1+ k_{focus}V_{focus})(1-(ripple/100) + random\ fluctuation) \quad (4)$$

These formulas are calculated in JavaScript functions in the energy range to generate spectrum data. The estimated values are exported to Chart.js graphs and updated in real time as user parameters change. Thus, students can numerically and visually experience how physical parameters shape the X-ray spectrum.

The dose calculation was developed to model the radiation effect of X-ray tube parameters on the patient and the environment. The room output dose is calculated by the interaction of variables such as tube voltage (kV), filament current (mA), exposure time (ms), distance between the patient and the tube (cm), and atomic number of the anode material (Z) (Equation (5)) [16].

$$D = \frac{kV.mA.ms.Z}{dist^2.1000} f_{filter}.f_{collimator} \quad (5)$$

$$H = \frac{kV.mA.ms}{1400} f_{dia}.f_{ref} \quad (6)$$

D is the dose (μGy), dist is the distance (cm), and f_{filter} and $f_{collimator}$ are the coefficients representing the filtration and collimator effects. Filtration reduces the dose by absorbing low-energy photons, while a collimator affects the dose distribution by shaping the beam. The patient dose was modeled as approximately 70% of the room exit dose.

The simulator records dose values as a time series and visualizes them with dynamic charts using the Chart.js library. These charts show in real time how the dose changes over the exposure time, and depending on parameter changes. In addition, statistical data such as average dose, maximum dose, and dose rate are calculated and presented to the user. In this way, students can numerically and visually analyze the relationship between dose and physical parameters.

The heat generated at the anode and the temperature variation are important parameters in the safe operation of the X-ray tube. Heat accumulation is calculated depending on factors such as tube voltage (kV), filament current (mA), exposure time (ms), anode material, and anode diameter (Equation 7) [17].

$$H = \frac{kV.mA.ms}{1400} f_{dia}.f_{ref} \quad (7)$$

H is the heat accumulation (kHU), f_{dia} is a coefficient representing the effect of the anode diameter, and fref represents the cooling type's effectiveness (oil, water, air). The anode temperature T = 25 + (100 H/C) (°C) is calculated considering the heat accumulation and the heat capacity of the anode material. T is the anode temperature, C is the heat capacity of the anode material, and 25 is the initial temperature. The simulator calculates the anode temperature in real time and visualizes the heat accumulation with a color scale.

*Sorumlu Yazar/Corresponding Author: aakyuz@mehmetakif.edu.tr

ISSN: 2618-6055 / 9, (1), 94 – 106, 2025
DOI: 10.62301/usmtd.1707321

Heat accumulation and temperature values are recorded as time series and then displayed as graphs using the Chart.js library. This enables students to investigate in detail the thermal behavior of the anode and the effects of parameter changes on heat management. The simulator performs energy calculation and efficiency analysis to evaluate the X-ray tube's energy conversion processes and efficiency. Total energy (Joules) is calculated using tube voltage (kV), filament current (mA), and exposure time (ms) (Equation 8).

$$E_{total} = V.I.t \tag{8}$$

The X-ray efficiency (η) is proportional to the atomic number (Z) of the anode material and the tube voltage (kV) (Equation 9).

$$\eta = 9.10^{-10}.Z.\ kV.\ f_{filter}.\ f_{cat}.\ 100 \tag{9}$$

X-ray energy and heat are calculated using Equations (10) and (11).

$$E_{x\text{-}ray} = E_{total}.\ \eta/100 \tag{10}$$

$$E_q = E_{total} - E_{x\text{-}ray} \tag{11}$$

The code calculates the total energy by multiplying the tube voltage, current, and exposure time. The X-ray efficiency is determined by the formula using the atomic number of the anode material and the tube voltage; the effects of filtration and cathode material are also considered. The total energy is divided into X-ray energy and the remainder as heat energy according to the efficiency ratio. These values are visualized in pie and gauge charts using Chart.js and updated in the user interface. Thus, energy distribution and efficiency are tracked in real time.

The animation loop runs continuously with the requestAnimationFrame function and performs the following operations in each frame: static elements (glass tube, anode, cathode, etc.) are drawn, electrons and X-rays are moved and drawn, and the rotation angle of the anode is updated. Electron generation occurs randomly, depending on the filament current, and moving particles are cleaned up as they leave the screen. This cycle ensures that the simulation provides a real-time and fluid visual experience.

The interactive nature of the simulator is based on users changing parameters and instantly observing the results. This interaction is achieved through JavaScript event listeners. Event listeners, such as oninput or onchange, are assigned to each slider and select element. When the user changes a parameter, the corresponding event listener is triggered, and the refreshUI() function is called. This function updates all parameter values, redoes spectrum, dose, heat, and energy calculations, and the graphics. In addition, the trackParameterChanges() function is called to track the number of parameter changes and update the statistics. In this way, the effects of user changes on the simulation are instantly visualized, and an interactive learning experience is provided.

The function getHeatColor (temp, meltPoint) calculates a color scale based on the anode temperature and provides the color change of the anode in the animation, so that the temperature increase is visually expressed. The new Electron () function generates new electron particles emitted from the cathode, which are characterized by velocity, position, and phase, and are moved in the animation. The newXRay(x, y) function generates X-ray particles emitted from the anode surface, which move at random angles and velocities to increase the realism of the simulation. These functions enable the dynamic and interactive nature of the simulator, providing the user with a rich visual experience.

Table 1 lists some properties and constants in the code that are not directly adjustable parameters but affect the simulation's behavior.

ISSN: 2618-6055 / 9, (1), 94 – 106, 2025
DOI: 10.62301/usmtd.1707321

Table 1. Parameters and values used in the simulator [18]

Anode Materials	W (Tungsten)	Z (Atomic Number) = 74, K_{α} = 17.5 eV, K_{β} = 19.6 keV, Density = 10.2 g/cm^3, color = “#f1c40f” (Yellow), Heat Capacity = 300 j/kg^{0}C, Melting Point = 3422 ^{0}C
	Mo (Molybdenum)	Z (Atomic Number) =42, K_{α} = 59 eV, K_{β} = 67 keV, Density = 19.3 g/cm^3, color = "#2ecc71" (Green), Heat Capacity = 150 j/kg^{0}C, Melting Point = 2623 ^{0}C
	Rh (Rhodium)	Z (Atomic Number) = 45, K_{α} = 20.2 eV, K_{β} = 22.7 keV, Density = 12.4 g/cm^3, color = “#f1c40f” (Yellow), Heat Capacity = 180 j/kg^{0}C, Melting Point = 1964 ^{0}C
Cathode Materials	W (Tungsten)	Work Function = 4.5 eV Emission Efficiency = 1.0
	ThW (Tungsten with Thorium)	Work Function = 2.6 eV Emission Efficiency = 1.5
Glass Types	Lead	Transmittance = 0.85 Density = 4.5 g/cm^3
	Borosilicate Glass	Transmittance = 0.95 Density = 2.2 g/cm^3
Filter Materials	Al (Aluminum)	Linear Attenuation Coefficient = 0.15 Z (Atomic Number) = 13
	Cu (Copper)	Linear Attenuation Coefficient = 0.35 Z (Atomic Number) = 29
	Mo (Molybdenum)	Linear Attenuation Coefficient = 0.45 Z (Atomic Number) = 42
Cooling Types	Oil	Efficiency: 1.0 Maximum Cooling Rate = 10 kHU/s
	Water	Efficiency: 1.5 Maximum Cooling Rate = 15 kHU/s
	Air	Efficiency: 0.7 Maximum Cooling Rate = 5 kHU/s
Chart Settings	maxDataPoints	Maximum number of data points to be shown in time series charts = 20
Initial Anode Temperature	25 °C	

3. Results and Discussion

The simulator provides dynamic visualizations and illustrations that improve comprehension of the operation of the X-ray tube. The electron beam animation shows the trajectory of electrons from the cathode to the anode and precisely captures their movement, speed, and focusing effects. X-ray production and propagation are animated to show how electrons interacting with the anode generate rays emitted at various angles and speeds, allowing users to track the direction and intensity of the X-ray beam visually. The anode’s rotation is simulated based on its RPM value, with heat accumulation on its surface represented through color changes, which helps comprehend the risk of overheating. Additionally, filtration thickness, material, and collimator aperture are physically represented in the animation, making the shaping and filtering of the X-ray beam visually intuitive.

*Sorumlu Yazar/Corresponding Author: aakyuz@mehmetakif.edu.tr

ISSN: 2618-6055 / 9, (1), 94 – 106, 2025
DOI: 10.62301/usmtd.1707321

Regarding spectrum and dose analysis, the simulator computes and shows the Bremsstrahlung and characteristic X-ray spectra based on the anode material and tube voltage, allowing students to study the energy distribution and peak formation. Physical models calculate doses for patients and room exits in real time. Graphs show how dose changes with filtration, collimation, exposure time, and distance. Time series analysis tracks dose and heat accumulation over time, allowing users to analyze both immediate and long-term effects of parameter changes.

The heat and energy efficiency analysis includes calculating the anode's heat accumulation and temperature changes and visualizing how cooling type and anode diameter influence heat management. The distribution of electrical energy into X-ray production and heat loss is computed, providing insight into the device's efficiency. X-ray yield is calculated by considering anode material, filtration, and cathode properties and is displayed to aid in understanding efficiency factors.

Finally, the simulator incorporates statistical tracking and feedback features. It monitors how frequently students adjust each parameter, supporting evaluation of the experimental process. Information on simulation duration and total accumulated dose is provided to raise awareness about safety and performance. Graphical summaries consolidate the effects of all parameters, enabling students to interpret and reflect on their experimental results easily. The parameter settings and controls are detailed in Table 2.

The screen output of the simulation can be seen as a single page. However, it is given in parts here. Figure 1 shows the X-ray generation animation and the selection area for tube parameters. All parameters can be changed on the screen. The X-ray spectrum screen output is given in Figure 2. The X-ray spectrum graph details the energy distribution of X-rays, with the x-axis representing a continuous energy range from 0 keV up to the tube voltage (e.g., 120 keV), and the y-axis indicating the relative radiation intensity. The spectrum is calculated based on several factors: Bremsstrahlung, which is the continuous spectrum resulting from electrons colliding with the anode and is modeled by the formula $I(E) \propto E(E_0 - E)$, where E is the energy and E_0 is the maximum energy equal to the tube voltage; characteristic K_α and K_β lines, which are intense peaks at specific energy levels dependent on the atomic structure of the anode material; the filtration effect, where the filter material and thickness reduce the low-energy portion of the spectrum by absorbing low-energy photons; cathode thickness and focusing voltage, which fine-tune the overall intensity and shape of the spectrum; and current ripple, which introduces small fluctuations in the spectrum. Changes in parameters affect the spectrum as follows: increasing the tube voltage raises the maximum energy of the spectrum and makes the characteristic lines more pronounced; increasing filtration reduces low-energy photons, cutting off the lower end of the spectrum; and changing the anode material alters the energies and intensities of the characteristic lines.

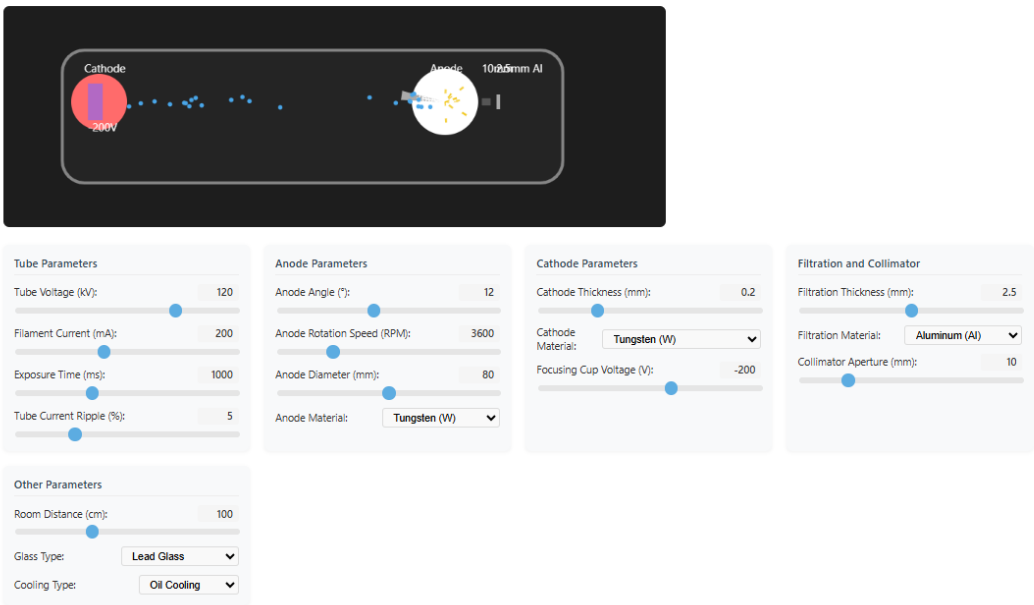

Figure 1. An animation showing the process of X-ray generation, along with a display of the parameter settings used

*Sorumlu Yazar/Corresponding Author: aakyuz@mehmetakif.edu.tr

ISSN: 2618-6055 / 9, (1), 94 – 106, 2025
DOI: 10.62301/usmtd.1707321

Table 2. Parameter settings, controls, and description

Parameter	Min	Max	Step	Description
Tube Voltage (kV)	40	150	5	Determines the energy at which electrons strike the anode. Students can observe the effect of voltage variation on the X-ray spectrum and dose.
Filament Current (mA)	10	500	10	This parameter controls the number of electrons leaving the cathode. As the current increases, the electron density and, therefore, the X-ray production increase. With this parameter, the effect of current on dose and heat accumulation can be analyzed.
Exposure Time (ms)	10	3000	10	Determines the X-ray generation time. A long exposure time leads to an increase in the total dose. Students can experience the effect of exposure time on dose and energy consumption.
Anode Angle (°)	6	20	0.5	It is the inclination angle of the anode surface. The anode angle affects the focusing and heat dissipation of the X-ray beam. The simulator visualizes the effect of anode angle on instrument performance.
Anode Rotation Speed (RPM)	1000	1200	100	Determines the speed of the rotating anode. High speed allows heat to spread over the anode surface and prevents overheating. Students can understand the role of rotation speed on heat accumulation.
Anode Diameter (mm)	40	120	1	Refers to the physical size of the anode. Anode diameter is related to heat capacity and durability. With this parameter, the thermal behavior of the anode can be studied.
Cathode Thickness (mm)	0.1	0.5	0.01	These parameters are effective on the structural properties and electron emission efficiency of the cathode. The choice of cathode material is important in terms of operating temperature and efficiency.
Filtration Thickness (mm)	0	5	0.1	It allows filtering of low energy photons from the X-ray beam. Filtration maintains image quality while reducing patient dose. Students can experience the filtration effect of different materials and thicknesses.
Collimator Aperture (mm)	5	30	1	Allows shaping of the X-ray beam. Collimator aperture affects dose distribution and image area.
Room Distance (cm)	50	200	5	It is the distance between the X-ray tube and the patient. As the distance increases, the dose decreases. With this parameter, the change of the dose depending on the distance can be analyzed.
Focusing Cup Voltage	-500	0	10	It affects the focusing of the electron beam. Focusing voltage variation affects the intensity of the electron beam and thus X-ray production.
Glass Type and Refrigeration Type				The permeability of the tube glass and the cooling method of the anode are simulated to analyze the durability and performance of the device.

The dose analysis graph (screen output is shown in Figure 3) displays dose values over simulation time, with the x-axis representing time in seconds and the y-axis showing dose measured in microgray (μGy). Two lines are plotted: the room exit dose and the patient dose. Dose calculation depends on several parameters, including tube voltage, current, exposure time, distance, and filtration. The patient dose is modeled as approximately 70% of the room exit dose. The collimator aperture directly influences the dose, with larger apertures increasing the dose. Additionally, the dose decreases with increasing distance according to the inverse square law. Changes in parameters affect the dose as follows: increasing

ISSN: 2618-6055 / 9, (1), 94 – 106, 2025
DOI: 10.62301/usmtd.1707321

voltage, current, or exposure time raises the dose; increasing filtration thickness or distance reduces the dose; and widening the collimator aperture increases the dose. The dose graph responds in real time to parameter adjustments, showing dose accumulation over time.

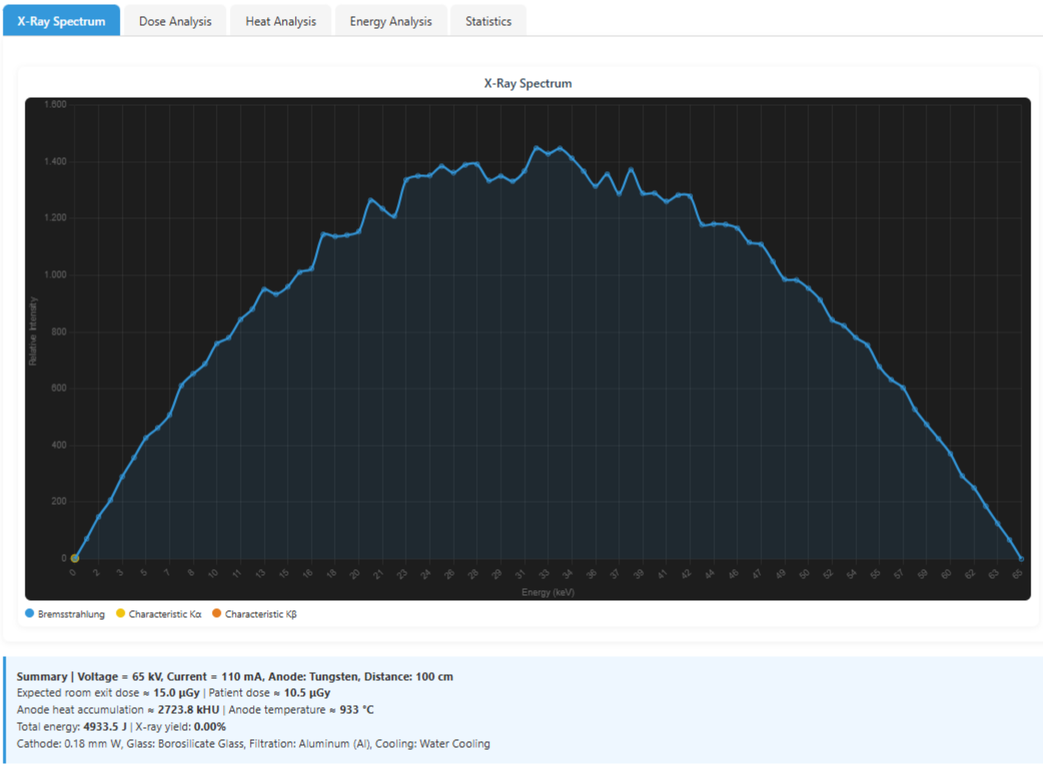

Figure 2. A screen output displaying the X-ray spectrum and its characteristics

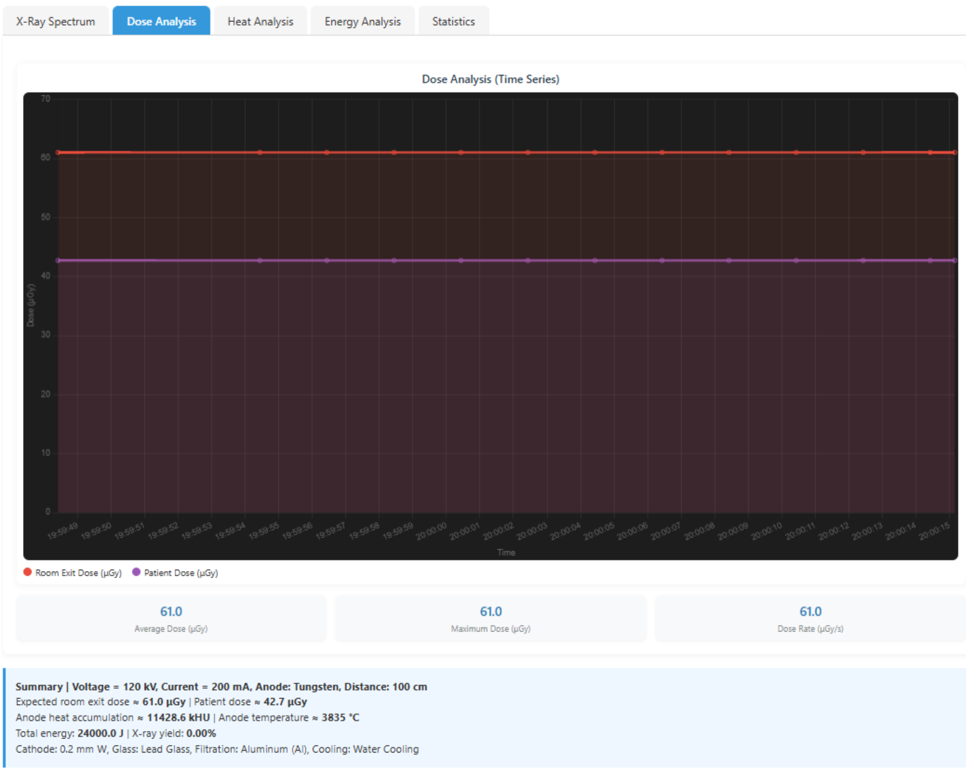

Figure 3. A screen output showing a graph of the dose analysis results, illustrating the distribution and levels of radiation dose

The heat analysis graph (screen output is shown in Figure 4) presents simulation time on the x-axis. It features two y-axes: the left y-axis shows heat accumulation measured in kilo heat units (kHU), while

ISSN: 2618-6055 / 9, (1), 94 – 106, 2025
DOI: 10.62301/usmtd.1707321

the right y-axis displays the anode temperature in degrees Celsius (°C). Heat accumulation depends on tube voltage, current, exposure time, anode diameter, and the type of cooling used. The anode temperature is calculated based on the accumulated heat and the anode's heat capacity. The anode's rotation speed and diameter influence how heat spreads and dissipates. The cooling method, whether oil, water, or air, determines the rate at which the anode cools as voltage, current, and exposure time increase, heat accumulation, and anode temperature rise. Conversely, increasing the anode's rotation speed and diameter reduces heat buildup and slows temperature increase. Changes in cooling type affect the maximum anode temperature and cooling rate. This graph visually enables monitoring of the anode's risk of overheating during operation.

Figure 4. A screen output displaying a graph of the heat analysis results, showing temperature distribution and thermal behavior.

The energy analysis (screen output is shown in Figure 5) includes two main visualizations: a pie chart showing the distribution of total energy into X-ray energy and heat energy, and a gauge chart indicating the percentage of X-ray efficiency. The total energy is calculated using the formula E=VIt. The X-ray efficiency η is computed by the formula $\eta = 9.10^{-10}.Z.\ kV$, where Z is the atomic number of the anode material and kV is the tube voltage; this value is adjusted based on filtration and cathode material effects. Heat energy is determined by subtracting the X-ray energy from the total energy. Parameter changes affect the analysis such that increasing voltage and selecting different anode materials raise X-ray efficiency, while filtration and cathode material also influence efficiency. Both the pie and gauge charts update in real time to reflect these changes.

*Sorumlu Yazar/Corresponding Author: aakyuz@mehmetakif.edu.tr

ISSN: 2618-6055 / 9, (1), 94 – 106, 2025
DOI: 10.62301/usmtd.1707321

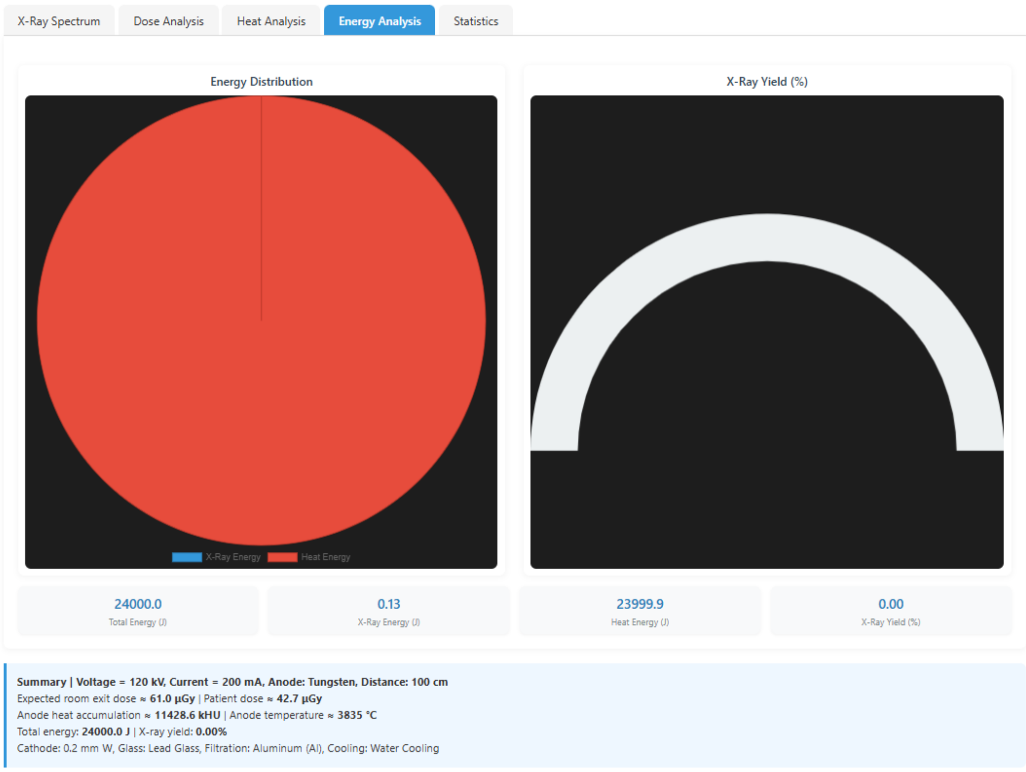

Figure 5. A screen output presenting the energy analysis results, including relevant data and visualizations

Figure 6. A screen output displaying a graph of statistical data, providing a visual representation of key metrics and trends

The statistics graph (screen output is shown in Figure 6) is a bar chart displaying the number of changes made to various parameters, including tube voltage (kV), filament current (mA), exposure time (ms), filtration, anode angle, and rotation speed (RPM). Alongside the chart, numerical indicators show the total number of parameter changes, the elapsed simulation time, and the accumulated total dose. Each time the user adjusts a parameter, the corresponding bar's value increases, providing a visual record of

*Sorumlu Yazar/Corresponding Author: aakyuz@mehmetakif.edu.tr

ISSN: 2618-6055 / 9, (1), 94 – 106, 2025
DOI: 10.62301/usmtd.1707321

interaction frequency. Meanwhile, the simulation time and total dose values update in real time, offering continuous feedback on the experiment's duration and radiation exposure.

4. Conclusion

Simulator offers a robust and interactive educational tool specifically designed for students in biomedical engineering and biomedical device technology. The simulator bridges theoretical knowledge and practical understanding by combining realistic animations of electron beams, X-ray generation, and anode rotation with detailed, real-time graphical analyses of X-ray spectra, radiation dose, heat accumulation, and energy efficiency. The ability to manipulate critical parameters such as tube voltage, filament current, filtration, and anode properties allows students to explore the complex interdependencies within X-ray tube operation safely and cost-effectively, without the risks associated with physical equipment. From an educational perspective, the simulator enhances learning by providing immediate visual and quantitative feedback, fostering active experimentation and critical thinking. Statistical tracking promotes reflective learning and safety awareness by assisting teachers and students in monitoring participation and parameter exploration. Students' conceptual understanding of X-ray physics is strengthened by this tool, which also gets them ready for practical uses in medical imaging and device maintenance. Overall, the simulator is a great addition to biomedical device technology curricula because it encourages practical learning, enhances technical proficiency, and reinforces safety principles crucial for aspiring industry professionals. The simulations' source codes are available on GitHub (https://aliakyuz12.github.io/Interactive-X-Ray-Tube-Simulation/) and can be used for educational purposes.

5. References

[1] S.F. Keevil, Physics and medicine: a historical perspective, Lancet 379 (9825) (2012) 1517–1524.

[2] F. Nüsslin, Wilhelm Conrad Röntgen: The scientist and his discovery, Phys. Medica 79 (2020) 65–68.

[3] Y.M. Al-Worafi, Radiology and Medical Imaging Research in Developing Countries, in: Handbook of Medical and Health Sciences in Developing Countries: Education, Practice, and Research, Springer Int. Publ., Cham, 2024, pp. 1–29.

[4] J.G.J. Lftta, A.N.A.A. Zahra, A.H.J. Ashour, A.H.K. Nasser, A.N. Shanawa, X-Rays and Their Uses on The Human Body, Curr. Clin. Med. Educ. 2 (8) (2024) 91–115.

[5] M.S. Linet, et al., Cancer risks associated with external radiation from diagnostic imaging procedures, CA Cancer J. Clin. 62 (2) (2012) 75–100.

[6] M. Kurudirek, Effective atomic numbers and electron densities of some human tissues and dosimetric materials for mean energies of various radiation sources relevant to radiotherapy and medical applications, Radiat. Phys. Chem. 102 (2014) 139–146.

[7] S. Prabhu, D.K. Naveen, S. Bangera, B.S. Bhat, Production of x-rays using x-ray tube, J. Phys. Conf. Ser. 1712 (1) (2020) 012036.

[8] M.J. Yaffe, J.A. Rowlands, X-ray detectors for digital radiography, Phys. Med. Biol. 42 (1) (1997).

[9] C. Cao, et al., Emerging X-ray imaging technologies for energy materials, Mater. Today 34 (2020) 132–147.

[10] A.H. Zamzam, et al., A systematic review of medical equipment reliability assessment in improving the quality of healthcare services, Front. Public Health 9 (2021) 753951.

[11] A. Haleem, M. Javaid, R.P. Singh, R. Suman, Medical 4.0 technologies for healthcare: Features, capabilities, and applications, Internet Things Cyber-Phys. Syst. 2 (2022) 12–30.

[12] F. Albert, Principles and applications of x-ray light sources driven by laser wakefield acceleration, Phys. Plasmas 30 (5) (2023) 050902.

[13] M. Berger, Q. Yang, A. Maier, X-ray Imaging, in: Medical Imaging Systems: An Introductory Guide, 2018, pp. 119–145.

*Sorumlu Yazar/Corresponding Author: aakyuz@mehmetakif.edu.tr

ISSN: 2618-6055 / 9, (1), 94 – 106, 2025
DOI: 10.62301/usmtd.1707321

[14] H. Jung, Basic physical principles and clinical applications of computed tomography, Prog. Med. Phys. 32 (1) (2021) 1–17.

[15] M.K.M. Alharbi, A. Zhou, M. Naunton, R. Davidson, C. Makanjee, Innovations in X-ray tube design and instrumentation for conventional radiological applications: a scoping review, Imaging Sci. J. (2025) 1–16.

[16] J.A. Seibert, X-ray imaging physics for nuclear medicine technologists. Part 1: Basic principles of x-ray production, J. Nucl. Med. Technol. 32 (3) (2004) 139–147.

[17] T. Bashore, Fundamentals of x-ray imaging and radiation safety, Catheter. Cardiovasc. Interv. 54 (1) (2001) 126–135.

[18] National Center for Biotechnology Information, PubChem Element Information, https://pubchem.ncbi.nlm.nih.gov/element (accessed 26.05.25).

***Sorumlu Yazar/Corresponding Author:** aakyuz@mehmetakif.edu.tr